

ENHANCED CONTROL OF RADIATOR HEATING SYSTEM

by

**Milan R. RISTANOVIĆ^{a*}, Goran R. PETROVIĆ^a, Žarko M. ČOJBAŠIĆ^b,
and Maja N. TODORVIĆ^a**

^a Faculty of Mechanical Engineering, University of Belgrade, Belgrade, Serbia

^b Faculty of Mechanical Engineering, University of Nis, Nis, Serbia

Original scientific paper

<https://doi.org/10.2298/TSC18S5337R>

In this paper a radiator heating system of a building is considered. For the purpose of the heating system optimization, a mathematical model of the system is developed. The linear quadratic algorithm with integral action is proposed and analyzed. This solution has proven to be expensive. Further analysis of the model is done and a reduction of the order of the system is proposed. An inverse-based controller design approach for minimum-phase first order system is used to provide realizable controller in the form of proportional integral controller. Optimal parameters of the control algorithm parameters have been chosen by integral of time absolute error criterion, and also by metaheuristic optimization. According to the real heating demand, a simulation of the plant is performed. Proposed controllers were tested by numerical simulation for a typical winter day for geographical region of the building. It is shown that advanced performance can be achieved with optimized control systems, and that by controller optimization a significant reduction of the energy consumption is obtained without losing the indoor comfort. This has also proved to be more economical solution.

Key words: radiator heating system, control, controller optimization, robust stability

Introduction

During the operation of the central heating systems, due to change of climatic influences, (mainly of the outside temperature and wind speed), heating demands are changing steadily. Heat delivery from the boiler always has to adapt to the heating demands of the consumers. Heating demands are changing during the day, as well as during the season [1].

Following deregulations that took place in many countries over the last few decades, energy market has been rapidly evolving and bringing to the attentions of practitioners and researches the challenging problems. By introducing a directive Energy Performance of Buildings Directive (EPBD), European Union tries to ensure market mechanisms to improve the energy efficiency in buildings, in other words, to determine an economic value of the energy conservations [1, 2].

In this paper, a radiator heating system of an existing office building is considered. System consists of a three-stage electrical boiler and radiators. Due to annual and daily changes of heating demands it is necessary to match the heat delivery from the boiler. Central control of the heat capacity can be done in the following ways: by changing the supply water temperature

* Corresponding author, e-mail: mristanovic@mas.bg.ac.rs

keeping the constant water-flow rate, by changing the water-flow rate keeping the water temperature constant, and combined, by changing both the water temperature and the water-flow rate. It is proposed to control system using an industrial programmable logic controller (PLC) by the continuous control of the boiler heaters. For the purpose of the heating system optimization, a mathematical model of the heating system is developed. Mathematical model is used for the reduction of the plant's order and optimization of the controller parameters, in order to have good tracking of the set-point, disturbance rejection and satisfactory robust stability.

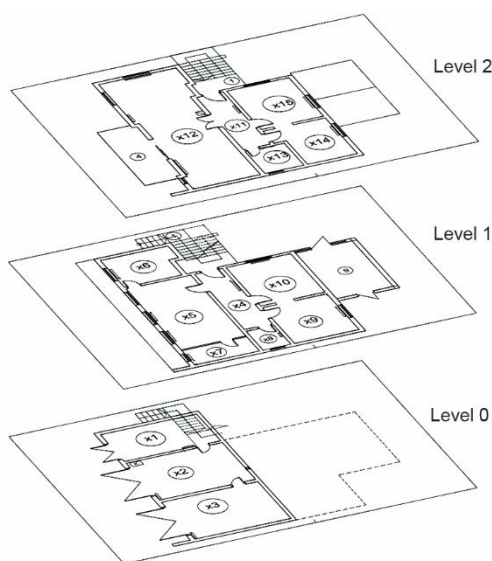


Figure 1. Axonometric view of the building

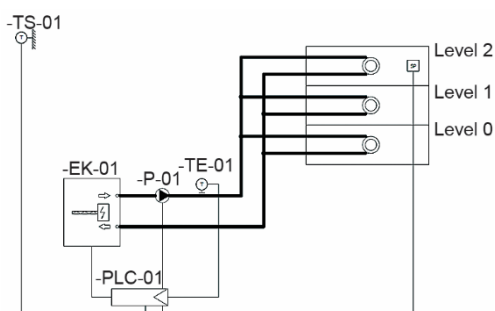


Figure 2. Functional schematics of the heating system

As it has been mentioned before, the building consists of 15 different rooms and the heating system. Each subsystem can be treated as a simple thermodynamic system that changes energy with the environment by thermodynamic action. By applying the First thermodynamic principle, as well as by introducing assumptions that all processes are performed on constant pressure and the working substance neither does perform work, nor work is done over it, it can be concluded that the change of internal energy, *i. e.* temperature of each room, depends only on the heat change with the environment. In this case, those relations, for r^{th} room, $r = 1, \dots, 15$, can be expressed mathemati-

System description

Building under consideration consists of 15 rooms in three levels, fig. 1. Internal temperature of each room represents one state variable in mathematical model, hence labels $x_i, i = 1, \dots, 15$, are introduced in fig. 1. Total net area is 270 m^2 . Ground level assumes garage and warehouse while other two levels are offices. Between ground and first level there is a non-heated room with unknown temperature, thus it is considered as a disturbance.

Functional schematics of the heating system is presented in fig. 2. Building is heated by an electrical boiler EK-01 of total power 24 kW. According to the outside temperature TS-01 and a heating curve, a desired value of inlet temperature TE-01 is determined. A slope, as well as an origin of the heating curve can be adjusted by a room thermostat unit SP. An industrial programmable controller PLC-01, according to an appropriate control algorithm, calculates control and controls the boiler and circulation pump P-01.

Mathematical modelling

Mathematical model in form of differential equations

cally by eqs. (1) and (2), depending on whether the thermodynamic system receives or gives energy:

$$\delta Q_{d,r} = \int_{t_1}^{t_2} \sum_{i=1}^n k_i A_i (T_f - T_{u,r}) \quad (1)$$

$$\delta Q_{q,r} = \int_{t_1}^{t_2} \sum_{j=1}^m k_j A_j (T_{u,r} - T_s) \quad (2)$$

where i is the specific radiator in the room, $i=1, \dots, n$, j – the specific wall through which the heat passes from the room, $j=1, \dots, m$, where n is number of radiators and m is number of walls. Further, k_i and k_j , [$\text{Wm}^{-2}\text{K}^{-1}$] denote particular heat transfer coefficients, while A_i and A_j denote areas of particular heat transfer areas [m^2]. Further, explicit expression for the internal energy change for r^{th} room, in differential shape, as a function of the fluid temperature in radiators T_f [K], outside temperature T_s [K], ceiling temperature T_c [K], floor temperature T_p [K], temperature of non-heated room T_{p9} [K], and internal temperature of the r^{th} room $T_{u,r}$ [K], can be derived as:

$$dU_r = \int_{t_1}^{t_2} \sum_{i=1}^n k_i A_i (T_f - T_{u,r}) - \int_{t_1}^{t_2} \sum_{j=1}^m k_j A_j (T_{u,r} - T_o) \quad (3)$$

$$\frac{dT_{u,r}}{dt} = \frac{\sum_{i=1}^n k_i A_i (T_f - T_{u,r}) - \sum_{j=1}^m k_j A_j (T_{u,r} - T_o)}{m_{v,r} c_{pv,r}} \quad (4)$$

where T_o [K] is the outside temperature.

Equation (4) can further be expanded by a room orientation and influence of the air infiltration:

$$\frac{dT_{u,r}}{dt} = \frac{\sum_{i=1}^n k_i A_i (T_f - T_{u,r}) - \sum_{j=1}^m O_r k_j A_j (T_{u,r} - T_s) - a_r l_r R_r H_r (T_{u,r} - T_s)}{m_{v,r} c_{pv,r}} \quad (5)$$

where $c_{pv,r}$ [$\text{kJkg}^{-1}\text{K}^{-1}$] is specific heat capacity of air in the r^{th} room, $m_{v,r}$ [kg] – the mass of air in the r^{th} room, O_r – the r^{th} room orientation coefficient, R_r – the r^{th} room characteristic, a_r [$\text{m}^3 \text{m}^{-1} \text{h}^{-1} \text{Pa}^{-2/3}$] – the infiltration of r^{th} gap, H_r – the building characteristic, and l_r [m] – the length of r^{th} gap.

Differential equation which describes change of fluid temperature as a function of boiler power, W [W] becomes:

$$\frac{dT_f}{dt} = \frac{1}{m_f c_f} \left[W - \sum_{r=1}^n k_i A_i (T_f - T_{u,r}) \right] \quad (6)$$

where c_f [$\text{kJkg}^{-1}\text{K}^{-1}$] is the fluid heat capacity, and m_f [kg] – the mass of the heated fluid.

Mathematical model in the state space form

The state space representation of the system yields an internal description of the system which may be useful if the model is derived from physical principles [3]. Using eqs. (5)

and (6), it is possible to determine mathematical model in form of differential equation for every single room.

In general, mathematical model of time-invariant MIMO plant, in the state-space form, is given by state equation and output equation:

$$\begin{aligned}\dot{\mathbf{x}}(t) &= \mathbf{A}\mathbf{x}(t) + \mathbf{B}\mathbf{u}(t) \\ \mathbf{y}(t) &= \mathbf{C}\mathbf{x}(t)\end{aligned}\quad (7)$$

where \mathbf{A} is the state-matrix, \mathbf{B} the input matrix, and \mathbf{C} the output matrix [4].

It is convenient to select the room temperatures and the fluid temperature as state variables:

$$\mathbf{x} = [T_{u,1} \quad T_{u,2} \quad T_{u,3} \quad \dots \quad T_{u,13} \quad T_{u,14} \quad T_{u,15} \quad T_f]$$
 (8)

Choice (8) leads to the system description in the state-space form based on eqs. (5) and (6):

$$\frac{dx_r}{dt} = \frac{\sum_{i=1}^n k_i A_i (x_{16} - x_r) - \sum_{j=1}^n k_j A_j (x_r - T_o)}{m_{v,r} c_{pv,r}}, \quad r = 1, \dots, 15$$

$$\frac{dx_{16}}{dt} = \frac{1}{m_f c_f} \left[W - \sum_{r=1}^{15} k_r A_r (x_{16} - x_r) \right]$$
 (9)

State-matrix is given by eq. (10), input matrix and output matrix are given by eq. (11), where plant input vector containing disturbances and control value is $(T_s \ T_c \ T_p \ T_{p9} \ W)^T$.

$$\mathbf{A} = \begin{bmatrix} -a_{11} & 0 & 0 & 0 & 0 & 0 & 0 & 0 & 0 & 0 & 0 & 0 & 0 & 0 & 0 & a_{116} \\ 0 & -a_{22} & 0 & 0 & 0 & 0 & 0 & 0 & 0 & 0 & 0 & 0 & 0 & 0 & 0 & a_{216} \\ 0 & 0 & -a_{33} & 0 & 0 & 0 & 0 & 0 & 0 & 0 & 0 & 0 & 0 & 0 & 0 & a_{316} \\ 0 & 0 & 0 & -a_{44} & 0 & 0 & 0 & 0 & 0 & 0 & 0 & 0 & 0 & 0 & 0 & a_{416} \\ 0 & 0 & 0 & 0 & -a_{55} & 0 & 0 & 0 & 0 & 0 & 0 & 0 & 0 & 0 & 0 & a_{516} \\ 0 & 0 & 0 & 0 & 0 & -a_{66} & 0 & 0 & 0 & 0 & 0 & 0 & 0 & 0 & 0 & a_{616} \\ 0 & 0 & 0 & 0 & 0 & 0 & -a_{77} & 0 & 0 & 0 & 0 & 0 & 0 & 0 & 0 & a_{716} \\ 0 & 0 & 0 & 0 & 0 & 0 & 0 & -a_{88} & 0 & 0 & 0 & 0 & 0 & 0 & 0 & a_{816} \\ 0 & 0 & 0 & 0 & 0 & 0 & 0 & 0 & -a_{99} & 0 & 0 & 0 & 0 & 0 & 0 & a_{916} \\ 0 & 0 & 0 & 0 & 0 & 0 & 0 & 0 & 0 & -a_{1010} & 0 & 0 & 0 & 0 & 0 & a_{1016} \\ 0 & 0 & 0 & 0 & 0 & 0 & 0 & 0 & 0 & 0 & -a_{1111} & 0 & 0 & 0 & 0 & a_{1116} \\ 0 & 0 & 0 & 0 & 0 & 0 & 0 & 0 & 0 & 0 & 0 & -a_{1212} & 0 & 0 & 0 & a_{1216} \\ 0 & 0 & 0 & 0 & 0 & 0 & 0 & 0 & 0 & 0 & 0 & 0 & -a_{1313} & 0 & 0 & a_{1316} \\ 0 & 0 & 0 & 0 & 0 & 0 & 0 & 0 & 0 & 0 & 0 & 0 & 0 & -a_{1414} & 0 & a_{1416} \\ 0 & 0 & 0 & 0 & 0 & 0 & 0 & 0 & 0 & 0 & 0 & 0 & 0 & 0 & -a_{1515} & a_{1516} \\ a_{161} & a_{162} & a_{163} & a_{164} & a_{165} & a_{166} & a_{167} & a_{168} & a_{169} & a_{1610} & a_{1611} & a_{1612} & a_{1613} & a_{1614} & a_{1615} & -a_{1616} \end{bmatrix}$$
 (10)

$$\mathbf{B} = \begin{bmatrix} b_{11} & b_{21} & b_{31} & b_{41} & b_{51} & b_{61} & b_{71} & b_{81} & b_{91} & b_{101} & b_{111} & b_{121} & b_{131} & b_{141} & b_{151} & 0 \\ b_{12} & 0 & 0 & 0 & 0 & 0 & 0 & 0 & 0 & 0 & b_{112} & b_{122} & b_{132} & b_{142} & b_{152} & 0 \\ b_{13} & b_{23} & b_{33} & 0 & 0 & 0 & 0 & 0 & 0 & b_{103} & 0 & 0 & 0 & 0 & 0 & 0 \\ 0 & b_{24} & 0 & 0 & 0 & 0 & 0 & 0 & b_{94} & b_{104} & 0 & 0 & 0 & 0 & 0 & 0 \\ 0 & 0 & 0 & 0 & 0 & 0 & 0 & 0 & 0 & 0 & 0 & 0 & 0 & 0 & 0 & \frac{1}{m_f c_f} \end{bmatrix}^T = \begin{pmatrix} \mathbf{B}_d^T \\ \vdots \\ \mathbf{b}_u^T \end{pmatrix} \quad (11)$$

$$\mathbf{C} = [0 \ 0 \ 0 \ 0 \ 0 \ 0 \ 0 \ 0 \ 0 \ 0 \ 0 \ 0 \ 0 \ 0 \ 0 \ 0 \ 1]$$

Control algorithm synthesis

Set-point for fluid temperature is generated based on the outside temperature and heating curve. Fluid temperature is accordingly chosen as output variable to be controlled with the only control input available, which is boiler power.

Linear quadratic controller

Linear quadratic controller (LQI) with integral action employs the same idea as LQR with feedforward gain, but it can provide better performance in the presence of uncertainty and better disturbance rejection [5]. Block diagram of the system with one output value and one control value, controlled with LQI is given in fig. (3).

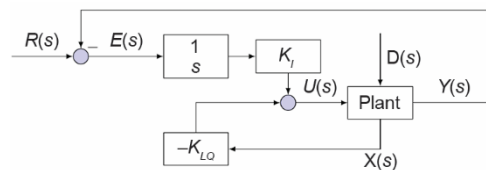


Figure 3. Block diagram of system with plant controlled with LQI

Introduction of the integral of error adds one more state to the system:

$$\dot{x}_{n+1}(t) = -e(t) = y(t) - r(t) \quad (12)$$

and this leads to the following state-space representation of the system:

$$\dot{\mathbf{x}}_e(t) = \begin{bmatrix} \dot{\mathbf{x}}(t) \\ \dot{x}_{n+1}(t) \end{bmatrix} = \begin{pmatrix} \mathbf{A} & \mathbf{0} \\ \mathbf{C} & 0 \end{pmatrix} \begin{bmatrix} \mathbf{x}(t) \\ x_{n+1}(t) \end{bmatrix} + \begin{pmatrix} \mathbf{b}_u \\ 0 \end{pmatrix} u(t) + \begin{pmatrix} \mathbf{0} & \mathbf{B}_d \\ -1 & \mathbf{0} \end{pmatrix} \begin{bmatrix} r(t) \\ \mathbf{d}(t) \end{bmatrix} \quad (13)$$

State vector, eq. (8), is extended with integral of the output error and is labeled with \mathbf{x}_e .

The LQI control law for particular plant is given by:

$$u(t) = -\mathbf{K}_{LQ} \mathbf{x}(t) + K_I \int_0^t e(\tau) d\tau \quad (14)$$

with vector of gains \mathbf{K}_{LQ} [WK^{-1}] and integral gain K_I [$\text{WK}^{-1}\text{s}^{-1}$].

Values of controller gains are found so that they minimize integral quadratic cost function:

$$J = \int_0^{\infty} [\mathbf{x}_e^T(t) \mathbf{Q} \mathbf{x}_e(t) + \rho u^2(t)] dt \quad (15)$$

Bryson's rule [6] presents good starting point for choice of square, positive definite, matrix Q and parameter $\rho > 0$. Since all states in the extended state vector are temperatures, with exception of the last, which is integral of temperature difference, it is reasonable from the physical point of view and for the sake of simplicity of analysis to choose matrix Q in eq. (13):

$$Q = qI \quad (16)$$

where I denotes identity matrix. For different values of parameters q and ρ , it is shown that the bigger the value of parameter q and the smaller value of ρ better set-point tracking is guaranteed in the sense of integral of time absolute error (ITAE). It is also confirmed, as well-known result for state-feedback control states, that gain margin for any value of parameters q and ρ will be infinite and phase margin will be greater than 60° , when all states are available, not estimated.

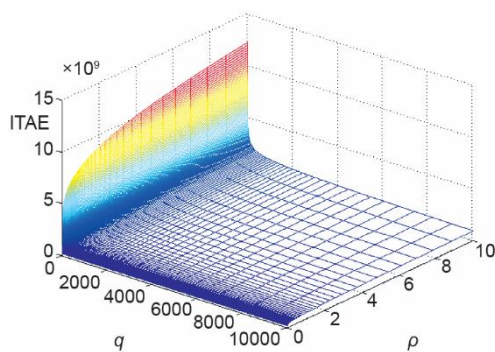


Figure 4. The ITAE as a function of q and ρ
(for color image see journal web site)

Optimal values of parameters chosen in this way also yield large control inputs. Since boiler power is limited, integrator anti-windup technique is implemented. Figure (4) shows values of integral of time absolute error as a function of parameters q and r in case of a standard winter day for given geographical location, for worst-case scenario initial conditions with integrator anti-windup technique implemented. The LQI control algorithm can provide good set-point tracking, but in order to implement it, information regarding all states has to be known.

The PI controller

System is not observable. Observability matrix rank is equal to five, and thus, there are 11 unobservable states. In order to avoid observability problem [7] additional measurements of state variables can be introduced in order to makes the system observable, but this choice makes the solution expensive.

Another way of solving this problem is to reduce the plant's order, find equivalent transfer function and design controller for only output feedback. Reduced model of plant, $G(s)$, has been found based on the step response similarity of the proposed second order reduced model and original model:

$$G(s) = \frac{9.828 \cdot 10^{-7} s + 1.469 \cdot 10^{-9}}{s^2 + 0.001981s + 3.66 \cdot 10^{-7}} \quad (17)$$

Similar result to eq. (17) can be obtained using optimal Hankel norm approximation, observing gaps in relative amplitudes of Hankel singular values.

Two systems can be described as close (*i. e.* have similar behavior) if their frequency responses are similar [3]. After the analysis of the Bode plot of the transfer function given by eq. (17), shown in fig. (5), it can be concluded that it is reasonable to further reduce model order, to obtain first-order transfer function.

The approximated first-order transfer function, $G_A(s)$, can be written in the form:

$$G_A(s) = \frac{K}{\tau s + 1} \quad (18)$$

with gain $K = 0.00401366$ [KW^{-1}] and time-constant $\tau = 4849.117$ [s].

Inverse-based controller design approach for minimum-phase first order system eq. (18) provides realizable controller in the form of PI controller, providing phase margin of 90° and maximum values of the sensitivity function $S(s)$ and complementary sensitivity function $T(s)$ equal to one [8]. As previously stated, if a controller is given by transfer function $G_C(s)$ as:

$$G_C(s) = \frac{\omega_c}{s} G_A^{-1}(s) = \frac{\omega_c}{K} \frac{\tau s + 1}{s} \quad (19)$$

then the open loop transfer function, $G_{OL}(s)$, becomes:

$$G_{OL}(s) = \frac{\omega_c}{K} \frac{\tau s + 1}{s} \frac{K}{\tau s + 1} = \frac{\omega_c}{s} \quad (20)$$

where ω_c [rads^{-1}], in this case determines value of the crossover frequency.

Transfer function of the standard PI controller, $G_{PI}(s)$, can be written in the well-known form:

$$G_{PI}(s) = \frac{K_P s + K_I}{s} \quad (21)$$

with proportional gain K_P [WK^{-1}], and integral gain K_I [$\text{WK}^{-1}\text{s}^{-1}$].

Comparing the transfer function, eq. (19), with the transfer function of the PI controller, eq. (21), it can be seen that following relations hold:

$$K_P = \frac{\omega_c}{K} \tau, \quad K_I = \frac{\omega_c}{K} \quad (22)$$

Using eqs. (18) and (19), closed-loop transfer function, $G_{CL}(s)$, becomes:

$$G_{CL}(s) = \frac{1}{\frac{s}{\omega_c} + 1} \quad (23)$$

Thus, it can be seen that controller parameters can be selected through choice of crossover frequency. Larger values of crossover frequency provide better set-point tracking and disturbance rejection. This value is limited with a control magnitude and robust stability specifications.

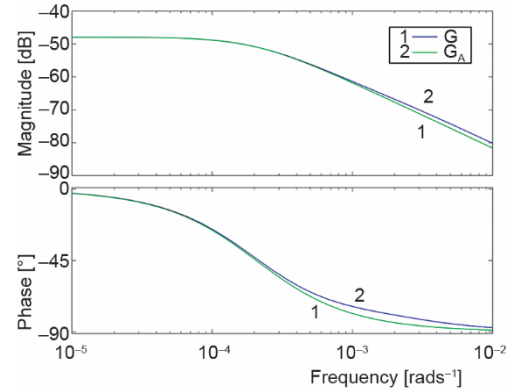


Figure 5. Bode plots of the identified and approximated plant transfer function

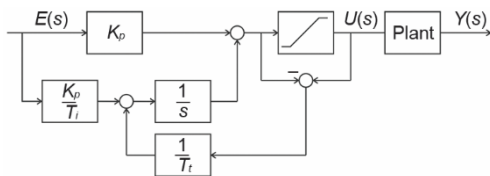


Figure 6. The PI controller with anti-windup

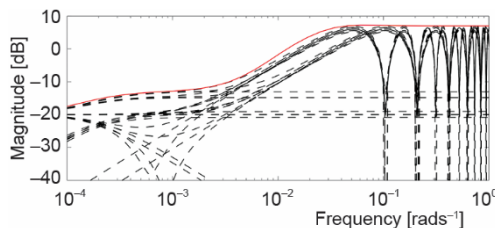


Figure 7. Magnitude plot of relative errors and relative uncertainty

value for long-period of time if fixed-structure controller is used and because of that proposed PI controller is extended by the anti-windup based on back-calculation. This controller architecture is shown in the fig. 6, where T_t [s] denotes tracking constant [8].

Perturbed approximated plant transfer function, $G'(s)$, can be written in a form of first-order plant with gain K' [KW^{-1}], time constant τ' [s], and time delay θ [s]:

$$G'(s) = \frac{K' e^{-\theta s}}{\tau' s + 1} \tag{24}$$

Figure (7) shows relative errors for 27 combinations of perturbed plant gain, time-constant, and time-delay. Relative uncertainty weight is chosen as:

$$w_1(s) = \frac{s + 9 \cdot 10^{-5}}{0.22387 + 0.0009 \left(\frac{s}{3.1622} + 0.005 \right)^2} \frac{(s + 0.005)^2}{644.725 s^2 + 42.556 s + 1} \frac{644.725 s^2 + 38.0872 s + 1}{644.725 s^2 + 42.556 s + 1} \tag{25}$$

and its magnitude plot is also shown in the fig. (7) in solid line.

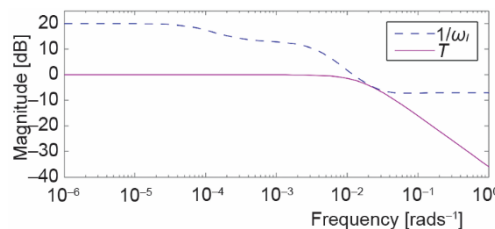


Figure 8. Bode plots of complementary sensitivity function and inverse of relative uncertainty

The rule of thumb for choice of the tracking constant in the PI controller with anti-windup suggests that its value should be around value for integral-time T_i . Considering eq. (22), it can be seen that $T_i = \tau$ and this enables us to choose a range for tracking constant worth considering in process of looking for optimal value.

Since a lot of assumptions have been used while deriving mathematical model, it is natural to consider robust stability of the closed loop. By experience, it is presumed that values for gain and time constant will be in the range of $\pm 10\%$ around the nominal values and the neglected delay shall not be greater than 60 seconds. Also, considering disturbance rejection, good design rule states that ω_c should be greater than $1/\tau$. Based on these considerations, range of interest for ω_c is $\omega_c \in [0.0002, 0.01667]$. Having in mind that plant has very large time constant, especially in the system-starting regime, until vicinity of the nominal working point is reached, control signal can potentially have upper saturation level

value for long-period of time if fixed-structure controller is used and because of that proposed PI controller is extended by the anti-windup based on back-calculation. This controller architecture is shown in the fig. 6, where T_t [s] denotes tracking constant [8].

Perturbed approximated plant transfer function, $G'(s)$, can be written in a form of first-order plant with gain K' [KW^{-1}], time constant τ' [s], and time delay θ [s]:

$$G'(s) = \frac{K' e^{-\theta s}}{\tau' s + 1} \tag{24}$$

Figure (7) shows relative errors for 27 combinations of perturbed plant gain, time-constant, and time-delay. Relative uncertainty weight is chosen as:

$$w_1(s) = \frac{s + 9 \cdot 10^{-5}}{0.22387 + 0.0009 \left(\frac{s}{3.1622} + 0.005 \right)^2} \frac{(s + 0.005)^2}{644.725 s^2 + 42.556 s + 1} \frac{644.725 s^2 + 38.0872 s + 1}{644.725 s^2 + 42.556 s + 1} \tag{25}$$

and its magnitude plot is also shown in the fig. (7) in solid line.

In fig. 8, complementary sensitivity function is shown together with inverse of the relative uncertainty weight.

From fig. 8, it is clear that further increasing of crossover frequency, which increases bandwidth, will not guarantee robust stability of the closed loop and this again confirms rightness of range for crossover frequency that should be taken into consideration. The rule of thumb for choice of the tracking constant in the PI controller with anti-windup suggests that its value should be around value for integral-time T_i . Considering eq. (22), it can be seen that $T_i = \tau$ and this enables us to choose a range for tracking constant worth considering in process of looking for optimal value.

Optimal values for parameters ω_c and T_t can be chosen using various criteria. In this paper, an ITAE has been used. Values of ITAE are shown in the fig. (9), where ω_c and T_t belong to the previously specified ranges. From fig. 9, it can be concluded that pair (ω_c, T_t) which provides least value for the ITAE for initial conditions in the worst-case system starting-regime scenario is (0.016, 4858.913).

System response is simulated for the typical winter model day. Namely, during the day, a 24-hour's outside temperature is used for the geographical position of the building, fig. 10.

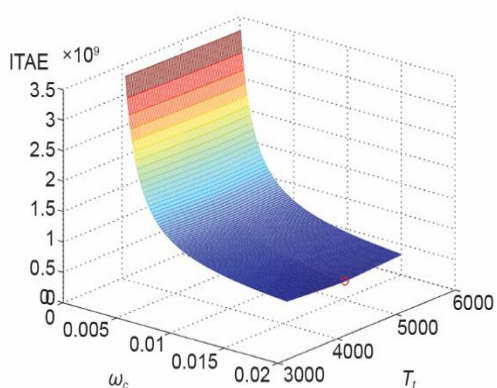


Figure 9. Integral of ITAE as a function of T_t and ω_c (for color image see journal web site)

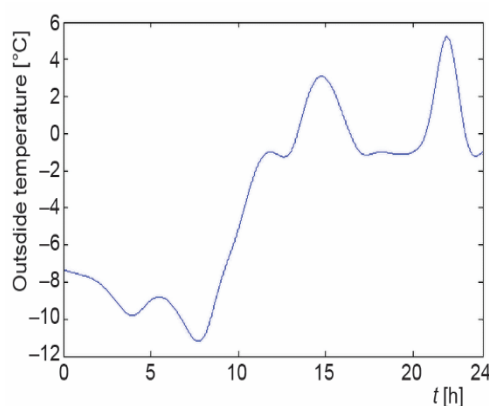


Figure 10. Outside temperature profile for a typical winter day

The outside temperature, combined with the heating curve, determines the real heating demand, *i. e.* set point for the controller. Results of numerical simulation can be seen in fig. 11. Set point fluid temperature is presented by blue line, while system output is shown by green line. It can be seen that for the worst scenario, output reaches the set point in 2 hours with no overshoot. During the numerical experiment, possible over-heating of the air temperature in rooms is limited to the 22 °C by thermal heads.

From the energy efficiency point of view, it is particularly important to have an information about the boiler power, in this case, control variable, fig. 12. The boiler operates with full power only during the heating up. As soon as the set point is reached, boiler operates with reduced power. Since the boiler is already in use for a few years, during the numerical simulation, the boiler power is intentionally limited on 20 kW because of possible calcium carbonate deposition.

Alternative controller tuning using metaheuristic optimization

Classical controller synthesis performed in chapter *The PI controller*, based on ITAE criterion, provides very good system performance which is verified in fig. 9. In order to try to further improve proposed PI controller, and even more important to propose procedure that would allow for additional future controller modifications such as non-linear controller implementation, an alternative controller parameters optimization has been attempted by use of metaheuristic optimization techniques.

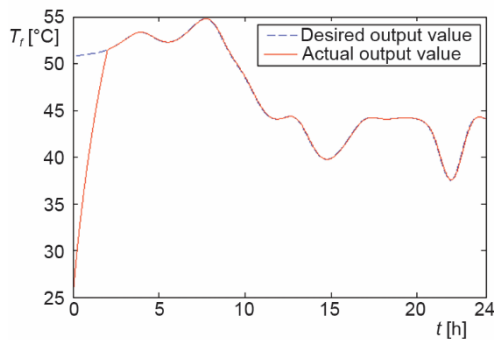


Figure 11. System response for a typical winter day

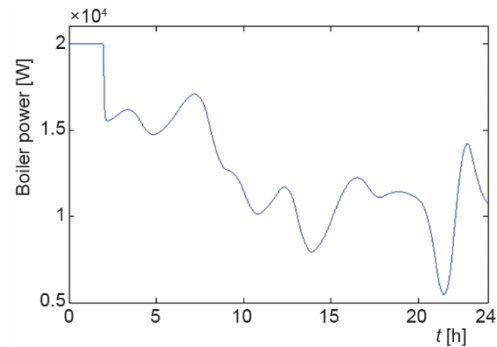


Figure 12. Boiler power

Therefore, the cost function to minimize tracking error has been defined:

$$J = \sum_{i=1}^N |e_i| = \sum_{i=1}^N |r_i - y_y| \quad (26)$$

where r is the reference variable (set point fluid temperature), y – the controlled output (fluid temperature), e – the control error, and N – the number of patterns. The goal of optimization is to adjust controller parameters, *i. e.* proportional and integral gains of PI controller (K_P and K_I), minimizing fitness (cost) function and thus improving controller performance by decreasing tracking error.

For controller optimization three metaheuristic techniques have been used: genetic algorithms (GA), simulated annealing (SA), and particle swarm optimization (PSO). The GA [9] are the most popular and widely used metaheuristic optimization technique, representing abstraction model of biological natural selection, based on Darwin's theory of evolution. The SA optimization was designed using analogy with metal annealing [9], and as other metaheuristic optimization algorithms is a technique possessing main ability to avoid being trapped in local optima unlike deterministic optimization techniques. Finally, the PSO is a technique developed on resembling swarm behavior, such as fish and bird schooling [9].

In each of the considered metaheuristic optimization algorithms, performance depends on its parameters values, so parameters were carefully selected by performing numerous experiments. Obtained results of controller tuning are summarized in tab. 1.

Table 1. The PI controller parameters obtained by conventional and metaheuristic optimization

Optimization method	Controller gain, K_P	Controller gain, K_I	Fitness function (cumulative error, less is better)
ITAE	$1.9330 \cdot 10^4$	3.9864	40,638
GA	$2.4283 \cdot 10^4$	5.0077	40,286
SA	$4.4670 \cdot 10^4$	9.3110	39,557
PSO	$4.7900 \cdot 10^4$	9.9900	39,510

It is obvious from the results presented in tab. 1 that it was possible to further improve already very sophisticated and optimized controller tuned by conventional ITAE crite-

tion. Even more interesting, metaheuristic algorithms were capable of identifying other optimal subsets of controller parameters, not in the vicinity of the point identified by ITAE criterion, bearing in mind that gains of the controller needed to stay limited in order not to jeopardize system stability. Still, the most important conclusion is that metaheuristic optimization is feasible concept for thermal controller optimization, which allows for implementation of the significantly more complicated and possibly non-linear controllers [10] making considered heating system even more suitable for smart buildings of the future [11].

Conclusions

In this paper, control of a radiator heating system for an office building is considered. System is centrally controlled by a PLC, according to the outside temperature and heating curve. In order to design a control algorithm, mathematical model of the heating system has been developed. Mathematical model has been used for obtaining the reduced order transfer function, useful for controller design.

As a performance reference, LQI controller has been proposed firstly, but to reduce costs a simple PI alternative has been designed. Parameters of the PI controller have been tuned by both conventional and metaheuristic approach, in order to provide good tracking of time-varying set-point, keeping the robust stability. It has been shown that the boiler operates with full power only during the transient period. In normal operating condition boiler provides only necessary amount of energy.

Besides performed comparison of tuning of parameters of the PI controller by conventional ITAE criterion and metaheuristic approaches, comparison could include more classical PI/PID tuning methods such as Refined Ziegler–Nichols, step response-based tuning and others [12].

Acknowledgment

This research has been supported by the Ministry of Education, Science and Technological Development of Republic of Serbia under the projects TR 33047, TR35005 and TR 35016.

References

- [1] Todorović, M., Ristanović, M., *Efficient Energy Use in Buildings* (in Serbian) University of Belgrade, Belgrade, 2015
- [2] Laković, M., *et al.*, Numerical Computational and Prediction of Electricity Consumption in Tobacco Industry, *Facta Universitatis Series: Mechanical Engineering*, 15 (2017), 3, pp. 457-465
- [3] Skogestad, S., Postlethwaite I., *Multivariable Feedback Control: Analysis and Design*, Vol. 2., John Wiley and Sons, New York, USA, 2007
- [4] Ogata, K., *Modern Control Engineering*, Prentice Hall, Englewood Cliffs, N. J., USA, 1997
- [5] Astrom, K. J., Murray, R. M., *Feedback Systems: an Introduction for Scientists and Engineers*, Princeton University Press, Oxford, UK, 2010
- [6] Franklin, G. F., *et al.*, *Feedback Control of Dynamic Systems*, Addison-Wesley, Reading, Mass., USA, 1994
- [7] Brown, R. G., Patrick, Y. C. H., *Introduction to Random Signals and Applied Kalman Filtering: with MATLAB Exercises and Solutions*, John Wiley & Sons, New York, USA, 1997
- [8] Astrom, K. J., Hagglund, T., *PID Controllers: Theory, Design and Tuning*, Instrument Society of America, Research Triangle Park, N. C., USA, 1995.
- [9] Dučić, N., *et al.*, Optimization of the Gating System for Sand Casting Using Genetic Algorithm, *International Journal of Metalcasting*, 11 (2017), 2, pp. 255-265
- [10] Precup, R.-E., *et al.*, Grey Wolf Optimizer Algorithm-Based Tuning of Fuzzy Control Systems with Reduced Parametric Sensitivity, *IEEE Transactions on Industrial Electronics*, 64 (2017), 1, pp. 527-534

- [11] Manić, M., Amarasinghe, K., *et al.*, Intelligent Buildings of the Future: Cyberaware, Deep Learning Powered, and Human Interacting, *IEEE Industrial Electronics Magazine*, 10 (2016), 4, pp. 32-49
- [12] Mataušek, M. R., Kvaščev, G. S., A Unified Step Response Procedure for Autotuning of PI Controller and Smith Predictor for Stable Processes, *Journal of Process Control* 13, (2003), 8, pp. 787-800